Rapid Communications in Mass Spectrometry

WILEY

Rapid Communications in Mass Spectrometry

RESEARCH ARTICLE OPEN ACCESS

Isolation and Identification of Mercury–Dissolved Organic Matter Complexes in Mercury–Humic Acid Suspensions

Ghulam Hussain Qasim[1] | Lisa Harris[2] | Vaughn Mangal[2] | Mario Montesdeoca[1] | Svetoslava Todorova[1] | Charles Driscoll[1]

[1]Department of Civil and Environmental Engineering, Syracuse University, Syracuse, New York, USA | [2]Department of Chemistry, Brock University, St. Catharines, Ontario, Canada

Correspondence: Svetoslava Todorova (stodorov@syr.edu)

Received: 13 September 2024 | **Revised:** 23 November 2024 | **Accepted:** 23 December 2024

Funding: This material is based upon work supported by the National Science Foundation, under Grant No. 2023712. Financial support was also received in the form of an NSERC Discovery Grant (V.M.).

Keywords: dissolved organic matter | Hg-DOM complexes | high-resolution mass spectrometry | mercury | solid-phase extraction

ABSTRACT

Rationale: The complexation with dissolved organic matter (DOM) is a pivotal factor influencing transformations, transport, and bioavailability of mercury (Hg) in aquatic environments. However, identifying these complexes poses a significant challenge because of their low concentrations and the presence of coexisting ions.

Methods: In this study, mercury–dissolved organic matter (Hg-DOM) complexes were isolated through solid-phase extraction (SPE) from Hg–humic acid suspensions, and complexes were putatively identified using ultrahigh resolution Fourier transform ion cyclotron resonance mass spectrometry (FTICR-MS).

Results: Dissolved organic carbon (DOC) and total Hg analysis before and after SPE showed an increase in DOC:Hg ratio. The DOC:Hg ratio was lower in extracts from cartridges with silica structure bonded with hydrocarbon chains (C18) than priority pollutant (PPL) cartridges at circumneutral pH, indicating that C18 was more effective at extracting DOM complexed Hg. These results were confirmed with FTICR-MS analysis, where two Hg-DOM complexes were putatively identified from PPL extracts as opposed to eight from C18 (Winnow score > 75%). In addition, $C_8H_{13}HgN_2O_2S$, a molecular formula with a *m/z* ratio of 403.04, was identified across three separate extractions using a C18 cartridge, suggesting that the complexes were preserved during extraction and, presumably, electrospray ionization.

Conclusions: The results highlight the effectiveness of the methodology developed in this study—SPE coupled with FTICR-MS for isolating and identifying Hg-DOM complexes. This approach allows for the exploration of the elemental and structural composition of Hg-DOM complexes, which affects Hg speciation, bioavailability, and transformations in aquatic ecosystems.

Synopsis: A methodology was developed to identify Hg-DOM complexes at low concentrations to gain insight into mercury bioavailability, transformations, and transport in the environment.

1 | Introduction

In the environment, mercury (Hg) exists in both inorganic and organic forms. The organic form of Hg, methylmercury (MeHg), is of greatest concern because of its neurotoxicity and ability to transfer to the fetus through the placenta [1, 2]. Moreover, the bioaccumulation and biomagnification of MeHg through the aquatic food web poses health risks to humans and wildlife. The main route of exposure to humans is through fish and shellfish consumption. Both biotic and abiotic processes

mediate Hg methylation and demethylation processes in aquatic environments, which are influenced by the presence of dissolved organic matter (DOM) [3, 4]. DOM is complex and heterogeneous, with varying chemical composition and containing functional groups like quinone, carboxyl, amino hydroxyl, and thiols [5, 6]. In reducing environments, quinone-like structures in DOM can reduce oxidized and soluble Hg (II) to highly insoluble and volatile elemental Hg(0). Thiol functional groups have a high binding affinity with Hg that results in the formation of thermodynamically stable Hg-DOM complexes [7]. Low-molecular-weight organic acids like carboxylic can bind to Hg and facilitate cotransport under aerobic conditions [8, 9]. This binding of Hg with DOM in aquatic environments affects bioavailability.

Microbes that possess the *hgc*A and *hgc*B genes assimilate bioavailable Hg via passive diffusion and facilitated transport before methylation to MeHg [10]. Hg complexed with low-molecular-weight and aliphatic Hg-S complexes can diffuse through the cell membrane, making it readily available for methylation [11]. Abiotic MeHg production induced by solar radiation is also driven by the smaller sized fraction of DOM [4]. Similar to the methylation of Hg, demethylation is also influenced by the presence and complexation with DOM. Demethylation of MeHg within MeHg-DOM complexes has been reported through intramolecular energy transfer, radical interaction, and direct photolysis [12]. The DOM-mediated methylation and demethylation of Hg depend on the concentration, chemical composition, and aromaticity of DOM [13]. Therefore, insight into the molecular composition of Hg-DOM complexes is crucial for unraveling the factors that govern Hg transformations and fate in water bodies.

The spectroscopic techniques such as X-ray absorption near-edge structure (XANES), extended X-ray absorption fine structure (EXAFS), and Fourier transform infrared (FTIR) have been employed to study Hg interaction with reduced sulfur and carboxylic groups found in humic acid [14, 15]. However, these techniques have limited ability to characterize the structure of Hg-DOM complexes, focusing primarily on Hg binding with adjacent ligands. Recently, Chen et al. [16] identified Hg-DOM complexes and their chemical structures using ultrahigh resolution Fourier transform ion cyclotron resonance mass spectrometry (FTICR-MS). Successful detection of Hg-DOM complexes was achieved under DOC:Hg with ratios of 3.5×10^{-2} [8] and 3×10^{-4} [16], when the experimentally proposed optimal ratio was 5×10^{-3} [7]. Although high-resolution FTICR-MS provides molecular-level information of DOM with the potential to identify Hg-complexed DOM, the widespread application of FTICR-MS for detecting Hg-DOM complexes has been limited. This constraint is due to the concentrations of extractable Hg-DOM complexes often falling below the analytical detection limit of FTICR-MS. [16] In this study, we seek to address this limitation by preconcentrating Hg-DOM complexes using a solid-phase extraction (SPE) methodology. Using Hg–humic acid (Hg-HA) suspensions, we report on the conditions that enhance the preservation of Hg-DOM complexes during extraction and facilitate their identification during electrospray ionization (ESI).

2 | Methods

2.1 | Sample Preparation

In natural environments, the majority (50%–90%) of DOM is composed of humic and fulvic acids [17]. In this study, humic acid (HA, Sigma-Aldrich, MO, USA) was used as a surrogate for DOM because of its higher solubility at circumneutral pH, which is generally representative of most natural waters. A stock solution of Hg-HA suspensions was prepared in Milli-Q with a final concentration of 0.1-mg/L Hg and 0.6-g/L HA. The stock was diluted to a working concentration of 5-μg/L Hg and 30-mg/L HA before extraction. To investigate the effect of pH on the extraction of Hg-DOM complexes, working solutions were adjusted to pH 4, 6, 7, and 8 with 0.1 N HCl/NaOH.

2.2 | Solid-Phase Extraction and Preconcentration of Hg-DOM

SPE was performed using a semiautomatic 12-sample loading SPE system (EZSPE, Fluid Management Systems, Inc., Billerica, MA, Figure S1). Two different cartridges, C18 cartridges with silica structure bonded with hydrocarbon chains (C18) and priority pollutant (PPL) cartridges containing hydrophobic styrene divinylbenzene copolymer (Fluid Management Systems, Inc., Billerica, MA), were tested for the extraction efficiency of Hg-DOM complexes. The cartridges were conditioned immediately before extraction by passing a 5-mL acetone:hexane solution (1:1 volume), followed by 10-mL methanol (MeOH). Lastly, the cartridges were rinsed three times with 10-mL Milli-Q water to flush the remaining solvent to prevent the premature elution of samples (Figure 1, Step 2). The cartridges were kept damp during conditioning and extraction processes to avoid deactivation of sorption sites and preserve the efficiency of cartridges. Five hundred milliliters of Hg-HA suspensions was passed through the cartridges at a constant flow rate using the built-in vacuum pump and N_2 pressure in the EZSPE system to extract the Hg-DOM complexes (Figure 1, Step 3). Prior to drying the cartridges, the rinse bottles were filled with 25 mL of Milli-Q to rinse and extract any residual complexes left in the sample bottles.

After extraction, the cartridges were dried for 45 min with N_2 filled with 10-mL MeOH to elute Hg-DOM complexes. (Figure 1, Step 4). After 5 min, the eluent was collected in 60-mL receiving vials (Figure 1, Step 5). Instrument blanks were prepared with 500 mL of Milli-Q water and processed through the EZSPE system following the procedure described above. All the samples were extracted and measured in triplicates.

The extracted samples were preconcentrated to improve the detection of Hg-DOM complexes on the FTICR-MS (Figure 1, Step 6). MeOH in the eluent was evaporated under vacuum and N_2 pressure. The dried samples were stored at −20°C until further analysis. Before analysis, the dried complexes were reconstituted into 2-mL MeOH. An aliquot of 0.8 mL was used for FT-ICR analysis. The remaining 1.2 mL was dried under vacuum and N_2 pressure and dissolved in Milli-Q water for DOC and total Hg (THg) analysis (Supporting Information).

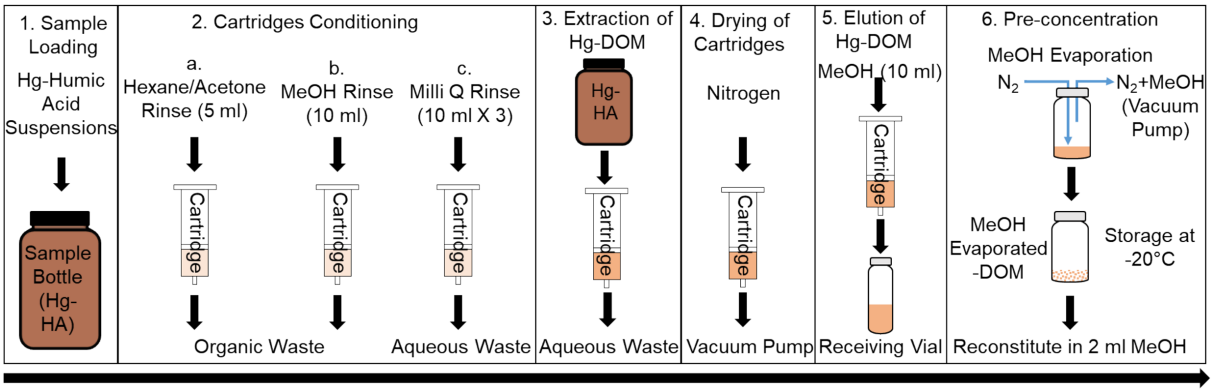

FIGURE 1 | Schematic diagram of solid phase extraction and preconcentration of Hg-DOM complexes isolated from Hg–humic acid (Hg-HA) suspensions. Solid-phase extraction was performed with C18 and priority pollutant (PPL) cartridges using EZSPE system (Fluid Management System, Inc.; Figure S1).

2.3 | Total Hg and DOC Analysis

THg was analyzed using the Tekran 2600 Automated Sample Analysis System following the USEPA method 1631, Rev. E [18]. DOC was measured by the TOC/DOC fusion system following the USEPA method 415.3 [19]. The precision and accuracy of the analysis were verified using standard reference materials (Standard Reference Material 1641d), duplicate samples, and spike samples. Instrument precision was established by analyzing continuing calibration verification and continuing calibration blank samples after every batch of 10 samples. The mean recovery of reference material was 96.5 ± 3.2, the relative percent difference for triplicate samples was ≤ 10%, and the average recovery of the continuous calibration verification samples was 97.1 ± 5.2%, all within the quality control criteria of the methods.

2.4 | OM Characterization and Hg Detection

A 7.0 T SolariX Fourier transform ion cyclotron mass spectrometer (Bruker; Germany) equipped with an ESI source in negation ionization mode was used for the characterization of Hg-DOM complexes. The methods used were similar to Mangal et al. [8] where 200 full mass scans of Hg-DOM complexes were acquired at 8 M resolution in negative ionization mode at a flow rate of 120 μL/h using a Hamilton syringe. A capillary voltage of 4400 V was used to acquire spectra between the 150–1000 mass to charge (m/z) range. The instrument was calibrated with sodium trifluoroacetate prior to sample acquisition with known m/z peaks between the 150–1000 m/z range. Accumulation times ranged from 0.20 to 0.35 s to acquire at least 10^9 ions before data acquisition. Generated spectra were converted from magnitude to absorption mode to enhance resolution and S/N ratios [20]. The Bruker Data Analysis software (v4.4) generated a list of m/z compounds, intensity, and resolution of each peak based on an S/N threshold of 4 using the FTMS function.

To detect Hg-containing compounds, the generated lists of m/z peaks were imported into the software Winnow [21] to detect seven isotopologues of Hg. Winnow generates a composite score summarizing potential matches to isotopes of a given compound based on m/z, intensity, and resolution. Scores closer to 100% represent more confident annotation. To remove false positive annotations of potential Hg complexes, only peaks with a Winnow composite score > 75% were utilized for subsequent analyses. In addition, the ratio ^{200}Hg:^{202}Hg was calculated in samples and compared with the theoretical ratio of 0.76 [8, 16]. In the current study, a Hg peak was considered significant if the experimental ratio of ^{200}Hg:^{202}Hg was > 0.55, within a 5-ppm error based on exact mass, and the Winnow score was > 75%. After identifying Winnow clusters of Hg-containing peaks, we used Bruker molweight formula software with elemental constraints $C_{1–50}$, $H_{1–100}$, $O_{1–30}$, $N_{0–4}$, $S_{0–3}$, and $P_{0–4}$. In addition, the isotope distribution patterns of theoretical versus experimentally derived spectra were manually checked for a given identification that met the above criteria to omit false positives. To confirm the molecules found, both ^{202}Hg and ^{200}Hg isotopes were added to the elemental constraints during the formula assignment using the Bruker Data Analysis software (v4.4). The raw elemental formula and Hg-DOM isotopologues data are provided in a spreadsheet as Supporting Information.

3 | Results and Discussion

3.1 | Isolation and Preconcentration of Hg-DOM Complexes

The Hg-HA suspensions prepared at pH 4, 6, 7, and 8 underwent SPE for the extraction of Hg-DOM complexes. The initial THg concentrations in Hg-HA suspensions were measured as 5 μg/L. The DOC concentration in Hg-HA suspensions increased with an increase in pH, with values of 3.8, 5.7, 8.1, and 8.8 mgC/L at pH 4, 6, 7, and 8, respectively (Figure S2). The decreased solubility of HA at lower pH was ascribed to increased hydrophobicity and protonation of carboxylic functional groups under acidic conditions, resulting in a decrease in negative surface charge on HA molecules and decreased electrostatic repulsion [22]. Note that precipitation was evident on cartridge filters, which increased with decreases in pH (Figure S2 inset). There was no significant difference observed in THg concentration extracted with both cartridges at pH 4, 6, and 8 ($p < 0.05$), but THg concentrations were higher in extracts from C18 than PPL at pH 7 (Figure S3b). Overall, Hg extracted from Hg-HA suspensions ranged from 0.5% to 1.3% of the spiked Hg. Presumably, not all the Hg spiked in humic acid solution was complexed with DOM. The HA used

in this study was not chemically or biologically reduced and the reduced HA has been reported to favor Hg complexation [23]. Moreover, Hg species analyzed in oligotrophic Wisconsin Lakes [24] and monimolimnion of meromictic Glacier Lake [25], USA, show that inorganic forms comprised more than 87.5% of THg. Thereby a major fraction of Hg in the Hg-HA suspensions may present as inorganic Hg (II). Although the percentage of Hg analyzed in extracts by the C18 and PPL cartridges appears low, it represents a substantial amount of organic Hg and is comparable with values reported for natural waters.

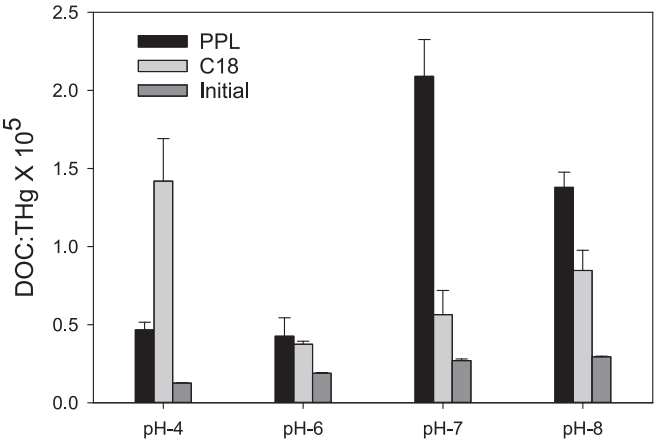

FIGURE 2 | Change in the molar DOC:Hg ratio in Hg–humic acid suspensions before and after solid-phase extraction calculated from Figure S3a.

The DOC extracted from Hg-HA suspensions ranged from 2.6% to 4.1% for the PPL and 1.3% to 13.5% for the C18 cartridge of initial DOC analyzed at pH 4, 6, 7, and 8 (Figures S2 and S3a). DOC extracted with PPL cartridges was 2.0, 1.5, and 1.1 times higher than the DOC extracted with C18 at pH 8, 7, and 6, respectively. This higher DOC extraction with PPL as compared with C18 might be attributed to the retention of both polar and nonpolar compounds by PPL, whereas C18 retains only nonpolar compounds [26]. At pH 4, DOC extracted with C18 was 3.3 times of PPL, likely due to the increased hydrophobicity of HA at low pH [27] and redissolution of precipitated nonpolar hydrophobic HA during MeOH elution. Our DOM extraction efficiency was low compared with other values reported in literature [26]. This lower efficiency is attributed to higher pH levels (4 and 6–8) of Hg-HA suspensions tested in this study, whereas in previous studies, natural samples were acidified to a pH of 2 before SPE. Moreover, the DOM in natural waters varies greatly in structural and chemical composition, whereas the DOM tested in this study consisted only of humic acid. We focused primarily on the extraction and preconcentration of Hg-DOM complexes at more circumneutral pH, as these conditions are more representative of natural waters. Moreover, under highly acidic conditions, proton competition for Hg binding sites leads to the breakdown of Hg-DOM complexes [28] and carbon chains through hydrolysis [29] potentially altering the structure and composition of these complexes.

The DOC to Hg mole ratios (DOC:Hg) in Hg-HA suspensions decreased with decreases in pH values (1.3×10^4 at pH 4 from 2.9×10^4 at pH 8), which was attributed to the precipitation of

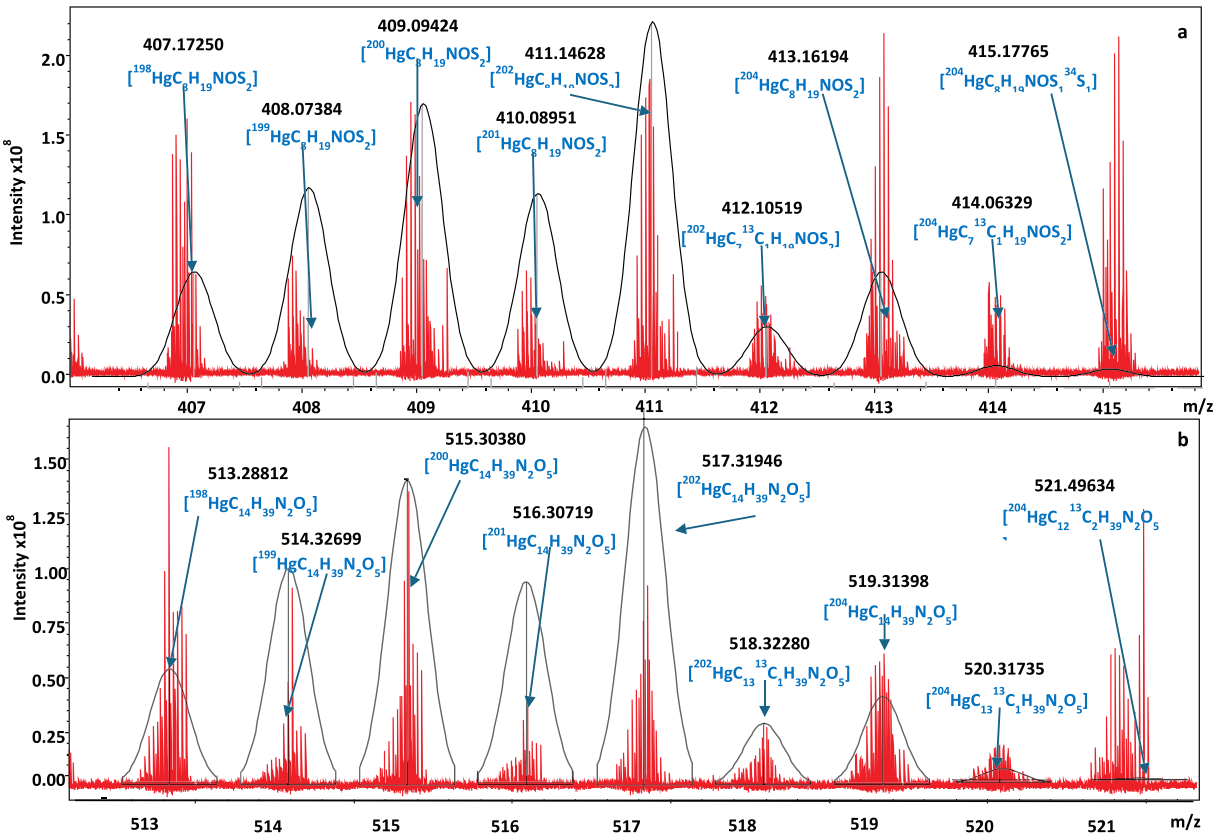

FIGURE 3 | Identified Hg-DOM complexes (red spectra) after extraction by PPL (a) and C-18 (b) cartridges and their respective theoretical isotopic distribution (black spectra) based on exact mass and isotopic conformation.

humic acid (HA) at lower pH levels. The DOC:Hg ratio increased significantly in all the extracts (Figure 2) and was 2.3–8.7 times higher with PPL and 2.0 to 11.3 higher with C18 than the initial DOC:Hg ratio. This increase in DOC:Hg ratio suggests that the cartridges retained the fraction of Hg that was complexed with DOM, whereas inorganic Hg was washed out during extraction. When comparing the two cartridges, extracts obtained with C18 at circumneutral pH (6–8) showed a lower DOC:Hg ratio. This pattern suggests that C18 retained only nonpolar Hg-DOM complexes.

3.2 | Identification of Hg-DOM Complexes

In Hg-DOM samples before SPE, no Hg-DOM peaks were confidently identified in the spectra acquired using FT-ICR-MS with Winnow scores above 75% at any pH (Figure S4). The highest aggregate score for Hg-DOM complexes in samples before extraction was 60%, where the presence of false positive peaks may arise [21]. The failure to confidently identify Hg-DOM peaks in samples before extractions suggests that the natural abundance of these complexes is quite low and presumably below the detection limit for FT-ICR-MS.

Following peak identification with Winnow scores > 75%, 10 Hg-containing DOM complexes were identified in Hg-HA extracts. Isotope simulation patterns confidently identified two Hg-DOM complexes using PPL extracts, whereas eight Hg-DOM complexes were identified with C18 cartridges (Figure 3). Among the eight complexes identified with C18 at pH 4, the molecule $C_8H_{13}HgN_2O_2S$ with a *m/z* ratio of 403.04 was confirmed across three separate extractions (Figure 4), based on Winnow scores and ^{200}Hg:^{202}Hg ratios similar to other identified complexes, suggesting that preferential identified complexes were retained during extraction and, presumably, ESI. The complexes identified with C18 at pH 4 had neutral masses ranging from 375 to 431. Similarly, complexes extracted with PPL had a neutral mass of 411 at pH 6 and 463 at pH 7. A decrease in mass at lower pH suggests the breakdown of carbon chains through hydrolysis [29]. When examining

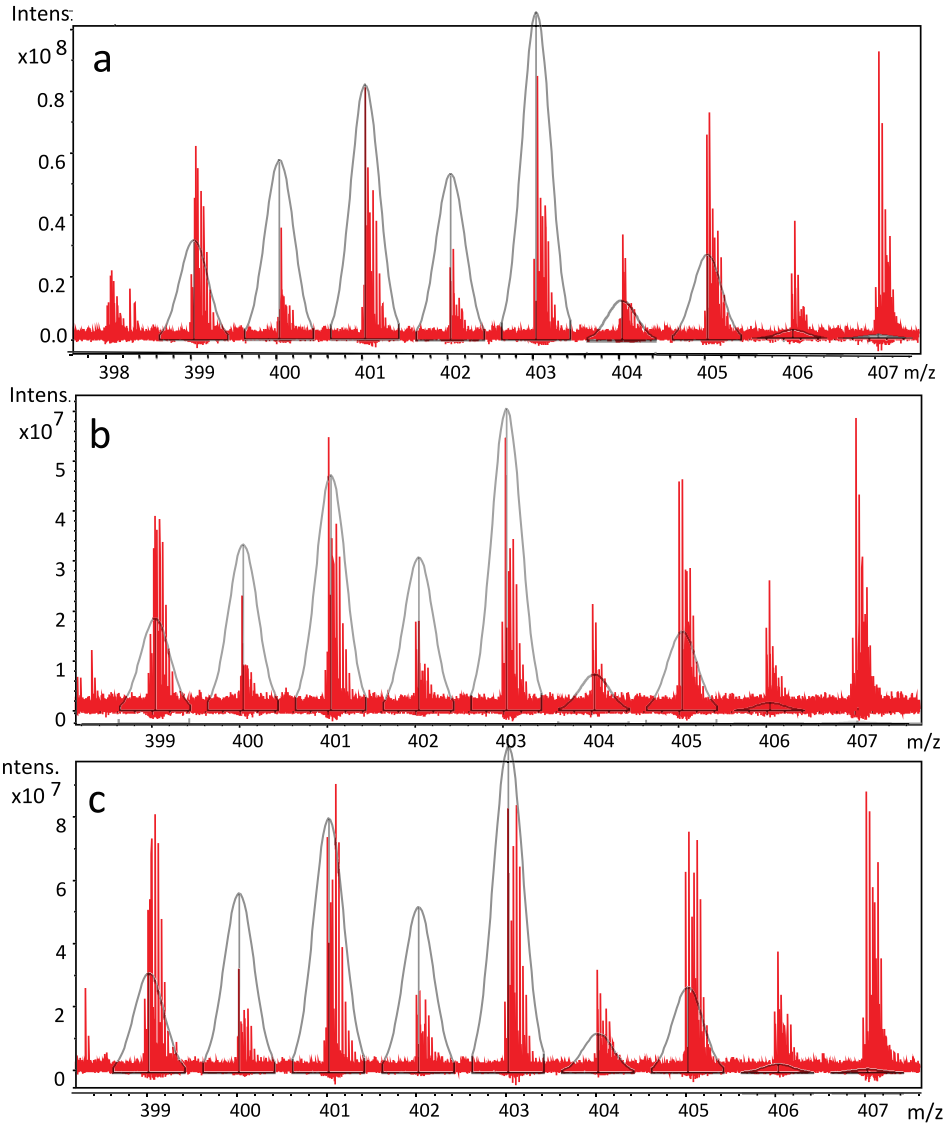

FIGURE 4 | Identified Hg-DOM molecular formula ($C_8H_{13}HgN_2O_2S$, 403.04042) was consistently identified after triplicate extractions (a,b,c) using C-18 cartridges at pH 4.

TABLE 1 | Hg-DOM complexes identified using FTICR-MS.

#	Cartridge Type	pH	Score	Neutral mass	Best molecular formula	m/z	Error (ppm)	O/C	H/C	DBE	AI_{mod}	NOSC
1	PPL	7	75.998	463.06	$C_{11}H_{19}HgNO_2S_2$	463.056	0.3	0.1818	1.7273	3	−0.1429	−0.7273
2		6	75.981	411.06	$C_8H_{19}HgNOS_2$	411.061	2.5	0.1250	2.3750	0	−0.7778	−1.25
3	C-18	4-a	79.883	431.04	$[C_9H_{15}HgN_2OP_2]^-$	431.037	0.7	0.1111	1.6667	4.5	0	−0.7778
4		**4-a**	**79.837**	**403.04**	**$[C_8H_{13}HgN_2O_2S]^-$**	**403.040**	**−2.2**	**0.25**	**1.6250**	**3.5**	**−0.1250**	**−0.1250**
5		4-a	75.652	485.05	$[C_{10}H_{22}HgO_3P_3]^-$	485.049	3.7	0.3	2.2	1.5	−0.5455	−1.6000
6		4-a	75.112	433.09	$[C_{10}H_{19}HgN_2O_2S]^-$	433.087	−2.3	0.2	1.9	2.5	−0.2500	−0.7000
7		**4-b**	**79.234**	**403.04**	**$[C_8H_{13}HgN_2O_2S]^-$**	**403.040**	**−1.7**	**0.25**	**1.6250**	**3.5**	**−0.1250**	**−0.1250**
8		4-b	77.530	417.06	$[C_9H_{15}HgN_2O_2S]^-$	417.056	−1.6	0.2222	1.6667	3.5	−0.1000	−0.3333
9		**4-c**	**79.058**	**403.04**	**$[C_8H_{13}HgN_2O_2S]^-$**	**403.040**	**−2.7**	**0.25**	**1.6250**	**3.5**	**−0.1250**	**−0.1250**
10		4-c	75.126	375.05	$[C_7H_{13}HgN_2OS]^-$	375.046	−3.5	0.1429	1.8571	2.5	−0.2857	−0.4286

Note: Bold highlighted (5, 8, and 10) are the duplicates identified in three replicates.

compositional characteristics of DOM presumably complexed with Hg, most DOM species were within $0.11 \leq O/C \leq 0.35$ and $1.63 \leq H/C \leq 2.78$ regions (Table 1). Based on conventional Van Krevelen diagram regions [30, 31], these molecules would be within the unsaturated hydrocarbon/low oxidized lignin region, suggesting that many of the OM molecules associated with Hg may resemble molecules with more hydrogenated compound classes. To infer the mobility and reactivity of identified Hg-DOM complexes, we calculated DOM proxies, including atomic ratios, double bond equivalence (DBE), aromaticity indices (AI_{mod}) [32], and the nominal oxygenation state of carbon (NOSC) [33]. The identified DOM molecules associated with Hg at pH 4 had DBE values ranging from 1.5 to 4.5, indicating multiple saturated double bonds (Table 1). AI_{mod} values ranging from −0.84 to 0 suggest relatively aliphatic DOM molecules with sulfur and oxygen functional groups that may participate in Hg complexation. In addition, negative NOSC values ranging from −1.64 to −0.13 suggest binding of DOM molecules that are generally found in reduced form and relatively thermodynamically accessible for microbial consumption [33, 34]. After eliminating false positives (Winnow scores > 75%), no Hg-DOM complex was identified from Hg-HA suspensions of pH 8 with either of the cartridges. This absence of spectra is likely attributed to the electrostatic repulsion between negatively charged Hg-DOM and sorbent material that limits the extraction of complexes during SPE at pH 4 and higher. At pH values greater than 4, carboxylic groups in humic acids deprotonate that result in a negative charge on humic acid surface [22].

Most of the C18 identified complexes contained sulfur heteroatoms, strong binding functional groups that form thermodynamically stable bonds with Hg (II). In comparison, the two Hg-DOM complexes identified after PPL extraction contained two sulfur molecules where $C_8H_{19}HgNOS_2$ was one of the most aliphatic complexes identified with an H/C ratio of 2.37 and an NOSC value of −1.25. Although there were no major differences between the molecular properties of Hg-DOM complexes, the number of confidently identified Hg-containing DOM complexes was greater for C18 than for PPL cartridges. Even though PPL cartridges have become the standard for DOM extractions, C18 cartridges tend to accumulate more nonpolar constituents [35] and preserve Hg complexes, as aromatic sulfur-containing DOM form more favorable bonds with Hg (II) [13].

4 | Summary and Implications

In the natural environment, Hg-DOM complexes exist at circumneutral pH values; however, these complexes occur at trace levels. Our results demonstrate that SPE effectively isolates and concentrates the Hg-DOM complexes at circumneutral pH. A decrease in pH can lead to the breakdown of these complexes through hydrolysis of carbon chain and analyzing Hg-DOM complexes at lower pH can underestimate the Hg-DOM complexes. In addition, we found the selection of cartridges is important for target Hg-DOM complexes. C18 cartridges were effective in preserving the complexes across replicates. In addition to DOC:Hg ratio, estimating the fraction of Hg complexed with DOM is crucial to assess the bioavailability and transport of Hg in natural systems. In this study, we

developed a methodology that effectively isolates and preserves Hg-DOM complexes at circumneutral pH and provides an innovative approach to studying the dynamic variability of Hg across ecosystems.

Author Contributions

Ghulam Hussain Qasim: investigation, formal analysis, visualization, writing – original draft, data curation. **Lisa Harris:** investigation, visualization, formal analysis. **Vaughn Mangal:** formal analysis, validation, writing – review and editing. **Mario Montesdeoca:** methodology, validation. **Svetoslava Todorova:** conceptualization, methodology, funding acquisition, project administration, writing – review and editing. **Charles Driscoll:** conceptualization, funding acquisition, writing – review and editing.

Acknowledgments

This material is based upon work supported by the National Science Foundation under Grant No. 2023712. Financial support was also received in the form of an NSERC Discovery Grant (V.M.). We would like to thank Mengyi Zhang for helping us with solid-phase extraction.

Data Availability Statement

The data that support the findings of this study are available from the corresponding author upon reasonable request.

References

1. R. A. Bernhoft, "Mercury Toxicity and Treatment: A Review of the Literature," *Journal of Environmental and Public Health* 2012 (2012): 1–10, https://doi.org/10.1155/2012/460508.

2. C. T. Driscoll, R. P. Mason, H. M. Chan, D. J. Jacob, and N. Pirrone, "Mercury as a Global Pollutant: Sources, Pathways, and Effects," *Environmental Science & Technology* 47, no. 10 (2013): 4967–4983, https://doi.org/10.1021/es305071v.

3. T. Barkay and B. Gu, "Demethylation—The Other Side of the Mercury Methylation Coin: A Critical Review," *ACS Environmental Au Journal* 2, no. 2 (2022): 77–97, https://doi.org/10.1021/acsenvironau.1c00022.

4. S. D. Siciliano, N. J. O'Driscoll, R. Tordon, J. Hill, S. Beauchamp, and D. R. S. Lean, "Abiotic Production of Methylmercury by Solar Radiation," *Environmental Science & Technology* 39, no. 4 (2005): 1071–1077, https://doi.org/10.1021/es048707z.

5. M. Ravichandran, "Interactions Between Mercury and Dissolved Organic Matter—A Review," *Chemosphere* 55, no. 3 (2004): 319–331, https://doi.org/10.1016/j.chemosphere.2003.11.011.

6. A. Manceau and K. L. Nagy, "Quantitative Analysis of Sulfur Functional Groups in Natural Organic Matter by XANES Spectroscopy," *Geochimica et Cosmochimica Acta* 99 (2012): 206–223, https://doi.org/10.1016/j.gca.2012.09.033.

7. M. Haitzer, G. R. Aiken, and J. N. Ryan, "Binding of Mercury (II) to Dissolved Organic Matter: The Role of the Mercury-To-DOM Concentration Ratio," *Environmental Science & Technology* 36, no. 16 (2002): 3564–3570, https://doi.org/10.1021/es025699i.

8. V. Mangal, T. Phung, T. Q. Nguyen, and C. Guéguen, "Molecular Characterization of Mercury Binding Ligands Released by Freshwater Algae Grown at Three Photoperiods," *Front Environmental Sciences* 6, no. JAN (2019): 155, https://doi.org/10.3389/fenvs.2018.00155.

9. A. Kutrowska and M. Szelag, "Low-Molecular Weight Organic Acids and Peptides Involved in the Long-Distance Transport of Trace Metals," *Acta Physiologiae Plantarum* 36, no. 8 (2014): 1957–1968, https://doi.org/10.1007/s11738-014-1576-y.

10. H. Luo, Q. Cheng, D. He, J. Sun, J. Li, and X. Pan, "Recent Advances in Microbial Mercury Methylation: A Review on Methylation Habitat, Methylator, Mechanism, and Influencing Factor," *Process Safety and Environment Protection* 170 (2023): 286–296, https://doi.org/10.1016/j.psep.2022.12.007.

11. M. Leclerc, D. Planas, and M. Amyot, "Relationship Between Extracellular Low-Molecular-Weight Thiols and Mercury Species in Natural Lake Periphytic Biofilms," *Environmental Science & Technology* 49, no. 13 (2015): 7709–7716, https://doi.org/10.1021/es505952x.

12. L. Y. Bin and Y. Cai, "Progress in the Study of Mercury Methylation and Demethylation in Aquatic Environments," *Chinese Science Bulletin* 58, no. 2 (2012): 177–185, https://doi.org/10.1007/S11434-012-5416-4.

13. R. A. Lavoie, M. Amyot, and J. Lapierre, "Global Meta-Analysis on the Relationship Between Mercury and Dissolved Organic Carbon in Freshwater Environments," *Journal of Geophysical Research – Biogeosciences* 124, no. 6 (2019): 1508–1523, https://doi.org/10.1029/2018JG004896.

14. U. Skyllberg, P. R. Bloom, J. Qian, C. M. Lin, and W. F. Bleam, "Complexation of Mercury (II) in Soil Organic Matter: EXAFS Evidence for Linear Two-Coordination With Reduced Sulfur Groups," *Environmental Science & Technology*. Published Online 40 (2006): 4174–4180, https://doi.org/10.1021/es0600577.

15. M. C. Terkhi, F. Taleb, P. Gossart, A. Semmoud, and A. Addou, "Fourier Transform Infrared Study of Mercury Interaction With Carboxyl Groups in Humic Acids," *Journal of Photochemistry and Photobiology A: Chemistry* 198, no. 2–3 (2008): 205–214, https://doi.org/10.1016/j.jphotochem.2008.03.018.

16. H. Chen, R. C. Johnston, B. F. Mann, et al., "Identification of Mercury and Dissolved Organic Matter Complexes Using Ultrahigh Resolution Mass Spectrometry," *Environmental Science & Technology Letters* 4, no. 2 (2017): 59–65, https://doi.org/10.1021/acs.estlett.6b00460.

17. E. M. Thurman, "Functional Groups of Dissolved Organic Carbon," in *Organic Geochemistry of Natural Waters* (Netherlands: Springer, 1985): 87–101, https://doi.org/10.1007/978-94-009-5095-5_4.

18. USEPA, "Method 1631, Revision E: Mercury in Water by Oxidation, Purge and Trap, and Cold Vapor Atomic Fluorescence Spectrometry Method 1631, Revision E: Mercury in Water by Oxidation, Purge and Trap, and Cold Vapor Atomic Fluorescence Spectrometry Method 1631, Revision E," (2002), accessed February 8, 2024, https://www.epa.gov/sites/default/files/2015-08/documents/method_1631e_2002.pdf.

19. B. B. Potter and J. C. Wimsatt, "Method 415.3 Measurement of Total Organic Carbon, Dissolved Organic Carbon and Specific UV Absorbance at 254 nNm in Source Water and Drinking Water," Vol 4 (2005), accessed February 8, 2024, https://cfpub.epa.gov/si/si_public_record_report.cfm?Lab=NERL&dirEntryId=103917.

20. Q. L. Fu, C. Chen, Y. Liu, M. Fujii, and P. Fu, "FT-ICR MS Spectral Improvement of Dissolved Organic Matter by the Absorption Mode: A Comparison of the Electrospray Ionization in Positive-Ion and Negative-Ion Modes," *Analytical Chemistry* 96, no. 1 (2024): 522–530, https://doi.org/10.1021/ACS.ANALCHEM.3C04651/ASSET/IMAGES/LARGE/AC3C04651_0004.JPEG.

21. M. C. Doran and K. L. LeBlanc, "A Computer Program to Simplify Analysis of Mass Scan Data of Organometallic Compounds From High-Resolution Mass Spectrometers," *Rapid Communications in Mass Spectrometry* 30, no. 23 (2016): 2561–2567, https://doi.org/10.1002/rcm.7748.

22. M. Brigante, G. Zanini, and M. Avena, "On the Dissolution Kinetics of Humic Acid Particles. Effects of pH, Temperature and Ca2+ Concentration," *Colloids and Surfaces A: Physicochemical and Engineering Aspects* 294, no. 1–3 (2007): 64–70, https://doi.org/10.1016/j.colsurfa.2006.07.045.

23. B. Gu, Y. Bian, C. L. Miller, W. Dong, X. Jiang, and L. Liang, "Mercury Reduction and Complexation by Natural Organic Matter in Anoxic Environments," *National Academy of Sciences of the United States*

of America 108, no. 4 (2011): 1479–1483, https://doi.org/10.1073/pnas.1008747108.

24. A. Mousavi, R. D. Chávez, A. M. S. Ali, and S. E. Cabaniss, "Mercury in Natural Waters: A Mini-Review," *Environmental Forensics* 12, no. 1 (2011): 14–18, https://doi.org/10.1080/15275922.2010.547549.

25. K. M. Yoshimura, S. Todorova, and J. F. Biddle, "Mercury Geochemistry and Microbial Diversity in Meromictic Glacier Lake, Jamesville, NY," *Environmental Microbiology Reports* 12, no. 2 (2020): 195–202, https://doi.org/10.1111/1758-2229.12823.

26. T. Dittmar, B. Koch, N. Hertkorn, and G. Kattner, "A Simple and Efficient Method for the Solid-Phase Extraction of Dissolved Organic Matter (SPE-DOM) From Seawater," *Limnology and Oceanography: Methods* 6, no. 6 (2008): 230–235, https://doi.org/10.4319/lom.2008.6.230.

27. L. H. Gan, Z. R. Yan, Y. F. Ma, et al., "pH Dependence of the Binding Interactions Between Humic Acids and Bisphenol A—A Thermodynamic Perspective," *Environmental Pollution* 255 (2019): 113292, https://doi.org/10.1016/J.ENVPOL.2019.113292.

28. M. Haitzer, G. R. Aiken, and J. N. Ryan, "Binding of Mercury (II) to Aquatic Humic Substances: Influence of pH and Source of Humic Substances," *Environmental Science & Technology* 37, no. 11 (2003): 2436–2441, https://doi.org/10.1021/es026291o.

29. H. Han, Y. Feng, J. Chen, et al., "Acidification Impacts on the Molecular Composition of Dissolved Organic Matter Revealed by FT-ICR MS," *Science of the Total Environment* 805 (2022): 150284, https://doi.org/10.1016/j.scitotenv.2021.150284.

30. S. Kim, R. W. Kramer, and P. G. Hatcher, "Graphical Method for Analysis of Ultrahigh-Resolution Broadband Mass Spectra of Natural Organic Matter, the Van Krevelen Diagram," *Analytical Chemistry* 75, no. 20 (2003): 5336–5344, https://doi.org/10.1021/AC034415P/ASSET/IMAGES/LARGE/AC034415PF00008.JPEG.

31. V. Mangal, N. L. Stock, and C. Guéguen, "Molecular Characterization of Phytoplankton Dissolved Organic Matter (DOM) and Sulfur Components Using High Resolution Orbitrap Mass Spectrometry," *Analytical and Bioanalytical Chemistry* 408, no. 7 (2016): 1891–1900, https://doi.org/10.1007/s00216-015-9295-9.

32. B. P. Koch and T. Dittmar, "From Mass to Structure: An Aromaticity Index for High-Resolution Mass Data of Natural Organic Matter," *Rapid Communications in Mass Spectrometry* 20, no. 5 (2006): 926–932, https://doi.org/10.1002/RCM.2386.

33. T. Riedel, H. Biester, and T. Dittmar, "Molecular Fractionation of Dissolved Organic Matter With Metal Salts," *Environmental Science & Technology* 46, no. 8 (2012): 4419–4426, https://doi.org/10.1021/es203901u.

34. O. J. Lechtenfeld, G. Kattner, R. Flerus, S. L. McCallister, P. Schmitt-Kopplin, and B. P. Koch, "Molecular Transformation and Degradation of Refractory Dissolved Organic Matter in the Atlantic and Southern Ocean," *Geochimica et Cosmochimica Acta* 126 (2014): 321–337, https://doi.org/10.1016/J.GCA.2013.11.009.

35. C. Y. A. Chuang and Y. H. Ho, "The Influence of Sources and Solid Phase Extraction Criteria on Dissolved Organic Matter Optical Properties in Aquatic Systems," *Frontiers in Marine Science* 10 (2023): 1140702, https://doi.org/10.3389/fmars.2023.1140702.

Supporting Information

Additional supporting information can be found online in the Supporting Information section.